Biochemical and Biophysical Research Communications 560 (2021) 139–145

Contents lists available at ScienceDirect

Biochemical and Biophysical Research Communications

journal homepage: www.elsevier.com/locate/ybbrc

MYOD modified mRNA drives direct on-chip programming of human pluripotent stem cells into skeletal myocytes

Giulia Selmin [a], Onelia Gagliano [b, c], Paolo De Coppi [a], Elena Serena [b], Anna Urciuolo [a, d], Nicola Elvassore [a, b, c, *]

[a] Great Ormond Street Institute of Child Health, University College London, WC1N1EH, London, UK
[b] Venetian Institute of Molecular Medicine (VIMM), 35129, Padova, Italy
[c] Industrial Engineering Department, University of Padova, 35131, Padova, Italy
[d] Molecular Medicine Department, University of Padova, Italy

ARTICLE INFO

Article history:
Received 16 April 2021
Accepted 28 April 2021

Keywords:
Pluripotent stem cell
Microfluidic
Myoblasts

ABSTRACT

Drug screening and disease modelling for skeletal muscle related pathologies would strongly benefit from the integration of myogenic cells derived from human pluripotent stem cells within miniaturized cell culture devices, such as microfluidic platform. Here, we identified the optimal culture conditions that allow direct differentiation of human pluripotent stem cells in myogenic cells within microfluidic devices. Myogenic cells are efficiently derived from both human embryonic (hESC) or induced pluripotent stem cells (hiPSC) in eleven days by combining small molecules and non-integrating modified mRNA (mmRNA) encoding for the master myogenic transcription factor MYOD. Our work opens new perspective for the development of patient-specific platforms in which a one-step myogenic differentiation could be used to generate skeletal muscle on-a-chip.

1. Introduction

Human organ-on-chip are being developed as a tool with useful applications in drug development and screening, as well as in disease modelling [1]. The availability of skeletal muscle on-chip models would benefit muscular-related disease research, helping in finding treatments for genetic disorders, such as dystrophies, in a cost- and time-effective manner. Significant advances have been made in the field of microfluidics and skeletal muscle models in the last years, which also included the use of multiple cell types and the application of mechanical or electrical stimulation [2].

Primary myoblasts are the most common cell type used for mimicking *in vitro* human skeletal muscle [2] although they have limited availability due to the need for donors, a remarkable batch to batch variation and the rapid senescence occurring *in vitro* restrict their use [3]. Both human embryonic and induced pluripotent stem cells (hESCs and hiPSCs) also offer a unique possibility of developing patient-specific *in vitro* models. This approach has a great potential for personalized medicine investigations like pharmacological testing, disease predisposition and modelling, as well as the development of optimized *in vitro* preclinical trials based on the genetic background of the specific patient [3].

A huge effort has been made in the last years for identifying protocols able to drive myogenic commitment and differentiation of hPSCs [4–11]. Protocols that start with mesoderm induction from hPSCs [5,7–11], revealed how this step is of primary importance and must be forced on hPSCs for reaching the myogenic commitment. Indeed, the chromatin state of hPSC is not permissive for myogenic transcription factors [12–14]. Alternative strategies for promoting myocyte derivation form hPSCs include the direct programming of the cells through the forced expression of key myogenic transcription factors (i.e. PAX3, PAX7 and MYOD) with both integrating [15–20] and non-integrating [21,22] programming methods. Despite the integrating programming systems show high efficiency of myogenic conversion, the risk of random insertional mutagenesis is a remarkable limitation [23]. Integration-free approaches for skeletal muscle differentiation can be achieved by using modified mRNAs (mmRNAs). Warren and colleagues provided the proof of concept that MYOD mmRNA was able to promote the programming of hiPSCs toward the myogenic lineage [21]. Despite the simplicity, controllability and non-mutagenic characteristics, this method is limited by the low efficiency of hPSC

* Corresponding author. Stem Cells & Regenerative Medicine Section, UCL Great Ormond Street Institute of Child Health, 30 Guilford Street, WC1N 1EH, London, UK.
E-mail address: n.elvassore@ucl.ac.uk (N. Elvassore).

https://doi.org/10.1016/j.bbrc.2021.04.129
0006-291X/

programming and the requirement of multiple transfections of the mmRNAs for a sustained expression of MYOD protein [22]. hPSCs have already been directly differentiated on-chip to multiple lineages such as cardiac [24,25], hepatic [25] and endothelial [26]. As regards the skeletal muscle, hPSCs-derived myocytes entirely developed on-chip has not yet been reported.

2. Material and methods

In this work, we aim at developing a strategy to efficiently differentiate human skeletal myocytes on-chip from hESCs and hiPSCs using microfluidic technology. In order to reach this goal, we combined the small molecules approach with a mmRNA technique. We initially established a protocol in which we successfully downscaled in microfluidic devices (μF) the conditions that induce hPSCs towards the mesendoderm lineage. Then, we transfected the mesendoderm-like cells with *MYOD* mmRNA for seven consecutive days. Moreover, upon the stimulation of terminal differentiation, hPSC-derived myocytes were competent to fuse together, forming multinucleated myotubes.

H9 hESCs line was obtained from WiCell Research Institute, USA. hiPSCs line was created in our laboratory through reprogramming of human fibroblasts from a healthy donor [33]. Microfluidic platform were fabricated as previously reported [25]. Mesoderm optimization experiments were performed in 96-well plates and in microfluidic platforms. Mesoderm-like cells were transfected with MYOD mmRNA (Stemgent) and nGFP (Miltenyi Biotec) once per day, for seven consecutive days starting from day 2 of differentiation.

Detailed material and methods are reported in the supplementary section.

3. Results

As first attempt, we tested whether *MYOD* mmRNA transfection could directly induce hPSCs differentiation toward the myogenic lineage. In this condition, only a very small amount of DESMIN-positive cells was detected inside the microfluidic channels (Suppl. Fig. S1A). Our results were in accordance with other studies, which showed that the forced exit of hPSCs from the pluripotent state and their priming toward paraxial mesoderm (premyogenic lineage) is of primary importance [12–14]. Hence, an initial comparison between multiwell (MW) and μF was performed to verify if in the two culture devices mesoderm induction was comparably effective after two days of mesoderm induction. HESCs showed different morphology in the two culture devices: in μF colonies were still easily distinguishable with compact centers but loose borders, whereas in MW the colony borders were broken, and cells spread out from them (Fig. 1A). Despite in both MW and in μF mesoderm induction allowed the production of BrachyuryT (T), immunofluorescence analysis also revealed that residual expression of the pluripotent marker OCT4 was particularly evident in μF, when compared to cells cultured in MW (Fig. 1B). Analysis of mRNA expression for the pluripotency markers *POUF5* (coding for OCT4) and *NANOG* confirmed an increased maintenance of pluripotent state in μF compared to MW. Mesodermal markers showed variable expression patterns, with *T* upregulated and *TBX6* downregulated in μF, compared to MW culture condition. *MSGN1* showed no significative difference in the two devices (Fig. 1C). These data not only demonstrate the importance of the initial mesoderm stimulation on the downstream myogenic differentiation efficacy, but also indicate the need of adjusting such initial step to our microfluidic setting in order to achieve the most permissive conditions able to promote myogenic programming through the subsequent *MYOD* mmRNA transfections. With the aim of optimizing this initial stimulation step and at the same time reducing the residual pluripotency in hESC-derived mesoderm-like cells in μF, culture conditions were modified considering two parameters: cell seeding density and CHIR concentration. A series of decreasing cell densities was investigated: 400, 200, 100 and 50 cells/mm^2. Two CHIR concentrations, 3 μM or 10 μM, were tested for each cell density (Fig. 1D and E). The morphological changes occurring after small-molecules treatment, in terms of colonies breaking and scattered cells, were noticeably different when considering the two CHIR concentrations. When 3 μM CHIR was used, cells from all the seeding densities remained in compact colonies. Instead, when 10 μM CHIR was used, morphologies comparable to those observed in MW were evident only on densities lower than 400 cells/mm^2 (Fig. 1D). In almost all the four cell seeding densities the mRNA levels of the well-known developmental regulator *T* at day 2 of induction were significantly higher for 10 μM CHIR treatment, compared to 3 μM CHIR. However, a remarkable decrease in residual pluripotency was detected by the quantification of mRNA levels of the pluripotency marker *NANOG*, which was downregulated in 10 μM CHIR treatment for cells seeded lower than 400 cells/mm^2 (Fig. 1E). In such culture conditions the mRNA levels of a key presomite marker, *MSGN1*, were significantly upregulated indicating a more successful paraxial mesoderm stimulation (Suppl. Fig. S1B). Overall, the qRT-PCR data corroborate on the molecular level the cell identity shift reflected by morphological changes. Furthermore, they emphasize the crucial role of cell density when inducing paraxial mesoderm *in vitro*. Given these results, 100 and 50 cells/mm^2 cell seeding densities were chosen, in combination with 10 μM CHIR, as the most effective early paraxial mesoderm inducing conditions in microfluidics.

We examined the mesoderm induction efficiency of CHIR treatment alone in comparison with CHIR + LDN on the optimized cell densities at D3. High efficiency was observed for both treatments in terms of percentage of cells expressing T at the protein level, independently from the initial cell density (Fig. 1F). However, CHIR + LDN treatment led to a significantly increased number of T-positive cells compared to 50 cells/mm^2 treated with CHIR alone (CHIR + LDN 100 cells/mm^2 = 98.73 ± 0.64%, CHIR + LDN 50 cells/mm^2 = 97.16 ± 2.47%, CHIR 50 cells/mm2 = 86.7 ± 2.32%, CHIR 100 cells/mm2 = 92.56 ± 6.56%; Fig. 1G). Moreover, this was accompanied by a significative downregulation of the residual pluripotency monitored with POUF5 (also known as OCT4) with CHIR + LDN and for all the cell seeding densities (Fig. 1H). Given the almost totality of T-positive cells and the lower levels of POUF5, the combination of CHIR and LDN was selected as the optimal treatment for the initial step of our myogenic differentiation protocol. The subsequent transfections with MYOD mmRNA were therefore performed on a mesendoderm-like cell population that had a reducing risk of residual pluripotency.

Previous to transfections on hPSCs, we ensured the efficacious translation and functionality of *MYOD* mmRNA. Human fibroblasts were the ideal cell type for such verification, given their chromatin state naturally permissive for MYOD without any prior mesoderm commitment requirement [28,29]. Exogenous MYOD was detected after a single transfection, confirming the presence of the protein and its correct nuclear localization (Suppl. Fig. S2A). Importantly, the resultant MYOD was also functional, as seen by the upregulation at mRNA level of its target gene *Myogenin* (*MYOG*) detectable 12 and 24 h after the transfection (Suppl. Fig. S2B).

We then investigated the effect of multiple *MYOD* mmRNA transfections on hESCs-derived mesendoderm-like cells obtained with our protocol optimized for microfluidics. Dramatic morphological changes occurred during the myogenic programming and the most striking differences emerged between transfected and non-transfected microfluidic channels, the latter used as control.

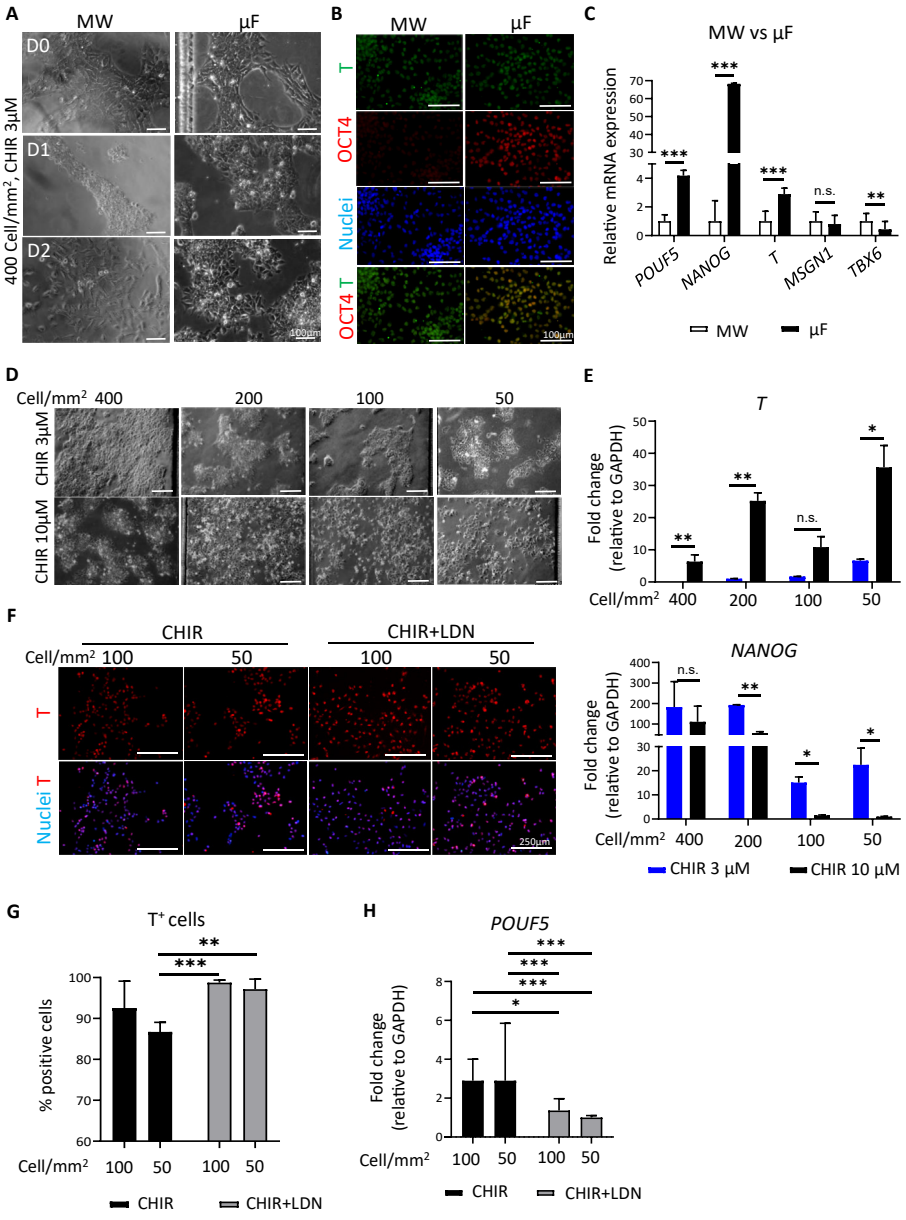

Fig. 1. Optimization of mesoderm induction in microfluidics. A. Bright field of hESCs seeded in multiwell and in microfluidic channels monitoring the cell morphology changes after the administration of CHIR for 48 h. B. Expression of the early mesendoderm marker T and the pluripotency marker OCT4 in both culture conditions at day 2. C. Relative mRNA expression of pluripotency and mesodermal markers in microfluidics compared to multiwell, at day 2. D. Different cellular morphologies depending on cell seeding number and CHIR concentration after 48 h of treatment. E. Expression of *T* and *NANOG* observed in correlation to initial cell seeding density and CHIR concentration. F. Immunofluorescence for T in hESCs seeded at 50 and 100 cell/mm^2 and treated with CHIR and CHIR + LDN. G. Quantification of T$^+$ cells for each condition. H. qPCR analysis of *POUF5* for each condition. * = $p < 0.05$; ** = $p < 0.01$; *** = $p < 0.001$.

Transfected cells started to show elongation at day 8 of differentiation (last day of transfection), becoming fully elongated at day 11, resembling the shape of myogenic cells. On the contrary, non-transfected controls showed no elongation throughout the differentiation (Fig. 2A). Such elongated myogenic-like morphology was therefore linked to *MYOD* mmRNA delivery and likely due to the MYOD-driven boost of the myogenic differentiation. Of note, cell morphology transition was similar for both the cell seeding densities considered. Modified mRNA encoding nucleus-targeted green fluorescent protein (nGFP) was included in the transfection mix with *MYOD* mmRNA and used to track the efficiency of the transfections. With this method transfections course can be monitored day by day for all their duration. The presence of GFP-positive cells confirmed successful mmRNA administrations (Suppl. Fig. 2C) and revealed a transfection efficiency ranging between 30% and 50%, independently from the initial cell density (Fig. 2B). Myogenic markers expression was analyzed at day 11. Such timepoint corresponds to 72 h after the last transfection, when any residual exogenous MYOD expression should result undetectable [21], indicating successful conversion of hPSCs to myogenic-like cells. When cells were screened for the presence of myogenic mRNAs, not only a significant upregulation of endogenous *MYOD* but also of *MYOG* and *MYHC3* (embryonic isoform) was documented in transfected cells at both cell density compared to controls (Suppl. Fig. S2D). However, when transfected channels were compared, *MYOD* and *MYOG* mRNA levels were significatively

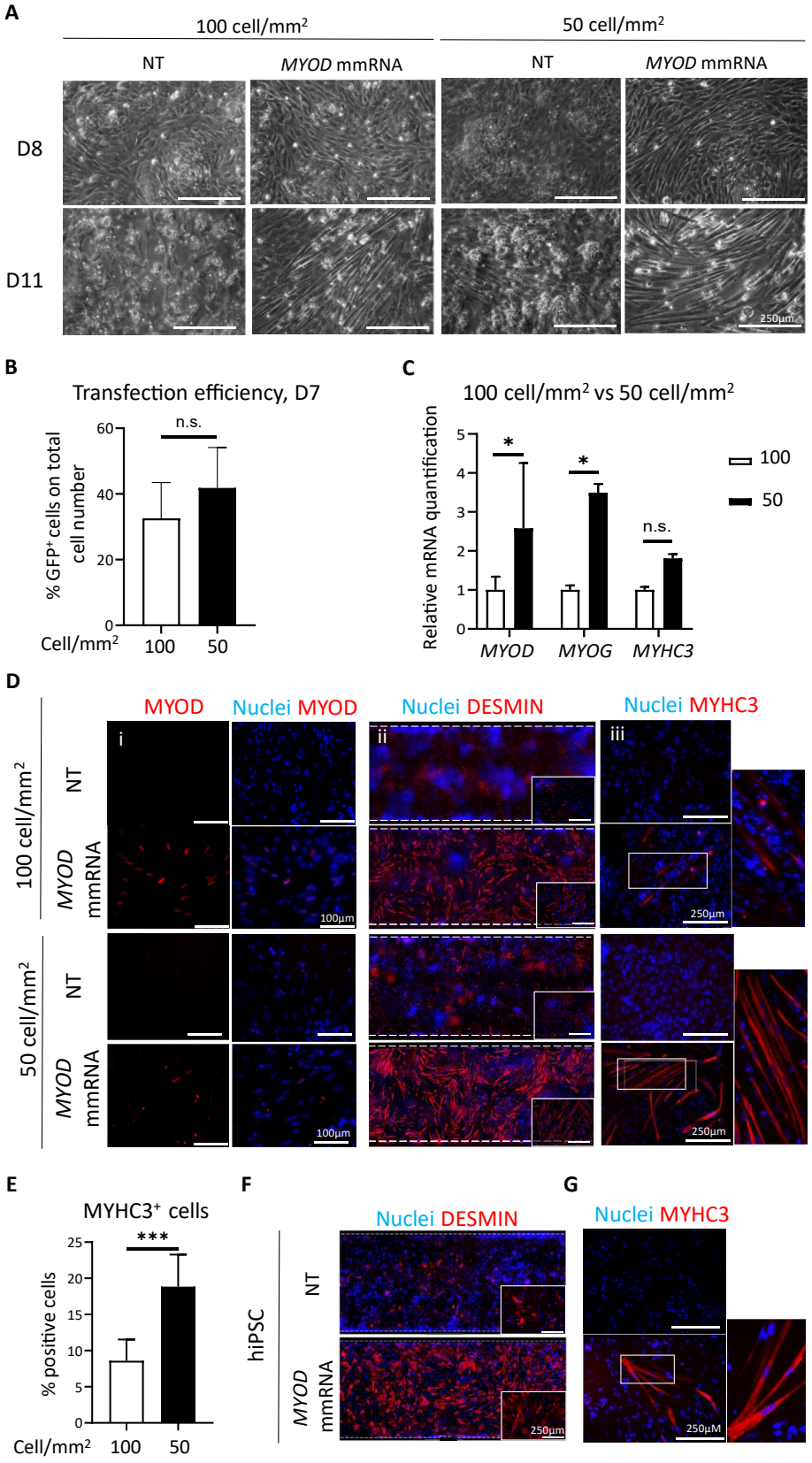

Fig. 2. MYOD mmRNA programming of mesendoderm-like cells derived from hPSCs. A. Representative images of the morphological changes occurring in non-transfected and transfected channels for the two selected cell seeding densities (hESCs). Spindle-like cells start to appear after D8 while a more evident elongated morphology emerge towards the end of the differentiation protocol (D11) following *MYOD*-mmRNA treatment. In non-transfected controls cells maintain a round morphological shape without showing any clear elongation. NT = non-transfected. B. Transfection efficiency calculated on GFP^+ cells at D7. C. qRT-PCR analysis of the endogenously expressed myogenic genes *MYOD*, *MYOG* and *MYHC3* at D11. D. Immunostaining of hESCs-derived myogenic cells at D11. i. Endogenous MYOD expression was detected only in transfected cells. ii) Channels sections showing homogeneous expression of $DESMIN^+$ cells, expressed in both controls and transfected channels. Dashed lines mark the channels' borders. iii) $MYHC3^+$ cells detected only in transfected channels. E. Quantification of $MYHC3^+$ cells at D11 for both initial cell seeding densities. F. Channels sections showing homogeneous expression of $DESMIN^+$ cells in both non-transfected and transfected hiPSCs-derived mesoderm-like cells at D11. G. $MYHC3^+$ cells detection at D11. * = $p < 0.05$; ** = $p < 0.01$; *** = $p < 0.001$.

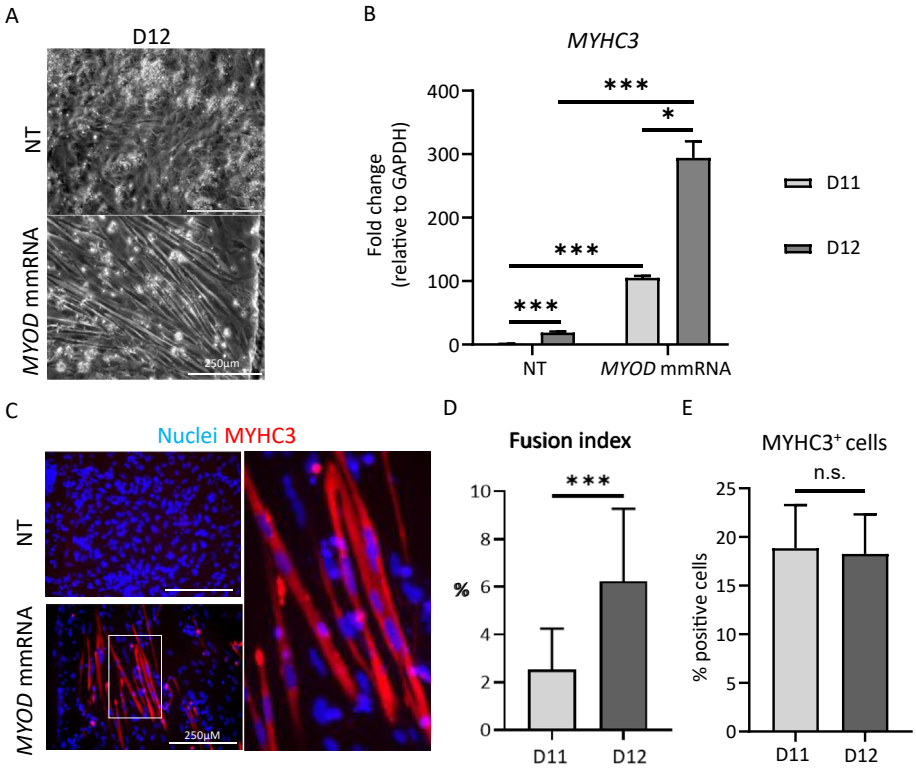

Fig. 3. Programmed myocytes on-chip are able to fuse into myotubes. A. Representative image of the morphology of non-transfected and transfected cells at D12. B. qPCR for *MYHC3* at D11 and D12. C. MYHC expressing multi-nucleated myotubes, detectable only in *MYOD* mmRNA-transfected channels. D. Fusion index calculated at d11 and D12. E. Quantification of $MYHC^{+}$ cells at D11 and D12. * = $p < 0.05$; ** = $p < 0.01$; *** = $p < 0.001$.

upregulated in 50 cells/mm^2. Instead, no statistically significative difference was observed for *MYHC3* mRNA levels (Fig. 2C). Cells expressing endogenous MYOD were detected in both cell densities exclusively in treated channels, confirming the presence of *MYOD* mmRNA-derived myogenic precursor cells (myoblast-like cells) (Fig. 2D–i). We found that remarkable differences in DESMIN-positive cells was evident between control and treated channels. In mmRNA-treated chips, cells were higher in number, displaying elongated morphology and homogeneously distributed all along the channels length (Fig. 2D–ii). Quantification of the number of DESMIN-positive cells confirmed this conclusion (Suppl. Fig. S2E). Similarly to the expression pattern observed for MYOD, also MYHC3 protein was detected solely in transfected cells (Fig. 2D–iii). Despite the equal *MYHC3* mRNA levels between the two cell densities, MYHC3 protein expression was significatively higher for 50 cells/mm^2 (100 cells/mm^2 = 8.6 ± 2.93%, 50 cells/mm^2 = 18.84 ± 4.44%, Fig. 2E). Hence, for the overall better myogenic differentiation obtained with such starting cell density, this experimental condition was selected for all the experiments that follow.

With the aim of verifying the efficacy of our protocol on different cell lines, we then investigated its feasibility on hiPSCs. Results similar to hESCs' myogenic induction were obtained, in terms of morphological changes and mesodermal and myogenic differentiation marker expression. Cells treated with CHIR and LDN were successfully primed towards the mesendoderm lineage, as seen by the spiky morphology and scattered distribution in the channels (Suppl. Fig. S3A) and the homogeneous expression of T at day 2 (Suppl. Fig. S3B). *MYOD* mmRNA-transfected hiPSCs-derived mesoderm-like cells exhibited an elongated cellular shape, less evident in non-transfected controls, following the same timing of hESCs (day 8 and day 11) (Suppl. Fig. S3C). The GFP-positive cells successfully detected during the transfections (Suppl. Fig. S3D) indicated a transfection efficiency of 32.58 ± 2.76% (Suppl. Fig. S3E). The distribution of DESMIN-positive cells at D11 evidenced once again the different amount of protein signal between control and transfected channels (48.27 ± 6.65% in controls, 62.32 ± 9.27% in treated channels) (Fig. 2F and Suppl. Fig. S3F). Upregulation of *MYHC3* mRNA levels was observed in *MYOD* mmRNA transfected cells compared to controls (Suppl. Fig. S3G) and was confirmed at the protein level (with 20% ± 6% of MYHC3-positive cells in treated channels and 0% MYHC3-positive cells in controls) (Fig. 2G and Suppl. Fig. S3H). Taken together, these data prove that in our microfluidic system a myogenic differentiation strategy relying solely on small molecules, even if proven successful in conventional culture conditions, is not sufficient to promote an adequate myogenic conversion of hPSCs in a short timeframe. In this scenario, *MYOD* mmRNA transfections are not only effective but also necessary to boost myogenesis. In fact, the myogenic phenotype is achieved in a shorter time (11 days) compared to traditional published protocols (30+ days) [4,7–9,15]. Our results also prove the feasibility and robustness of our myogenic strategy with different hPSCs lines.

Given the presence of MYHC3-positive cells in the microfluidic channels, we investigated whether such hESCs-derived myogenic-like cells could be further pushed to terminal differentiation promoting their fusion into multinucleated myotubes. Terminal differentiation was stimulated culturing cells in low serum conditions for 24 h starting at day 11, after which MYHC3 expression and the fusion index were examined. At day 12 cell morphology was similar to day 11, with transfected cells showing an elongated morphology, unlike non-transfected cells (Fig. 3A). A statistically significative upregulation of *MYHC3* mRNA levels at day 12 was seen when

comparing control and treated channels, and notably also when comparing transfected channels with those at day 11 (Fig. 3B). Despite the molecular increment, *MYHC3* expression in control channels was not enough to be detected at the protein level at day 12. Differently, in treated channels multi-nucleated MYHC3-positive myotubes were observed, demonstrating that our myogenic-like cells undertook a further differentiation stage after stimulation (Fig. 3C). Fusion index was calculated to be 6.24 ± 3.01%, significantly higher than day 11 (2.74 ± 1.71%) (Fig. 3D). It is important to emphasize that the amount of MYHC3-positive cells in transfected channels remained stable from day 11 to day 12 (day 12 = 18.26 ± 4.05, Fig. 3E), corroborating the fact that the higher fusion index at day 12 is not due to an increased number of MYHC3-positive cells but to the rearrangement of the myogenic-like cells into multi-nucleated myotubes. Taken together, these results demonstrate that our myogenic-like cells rapidly reach terminal myogenic differentiation when cultured in permissive conditions. Overall, our microfluidic devices coupled first with a small molecules-driven mesendoderm-induction step and then with a non-integrative skeletal muscle differentiation strategy efficiently program hPSCs into multi-nucleated myotubes without requiring any selection step and in a time as short as 12 days.

4. Discussion

The development of a one-step protocol to derive human myogenic cells from hPSCs in microfluidic devices results in a relevant physiological system for studying and modelling muscle-related diseases. Human ESCs and iPSCs are the ideal source for myogenic cells derivation. However, despite the development of many skeletal muscle differentiation protocols during the last decade [4,7–9,11,15,17,19,21,22,30], hPSC-derived myogenic cells on-chip have not yet been reported. In this scenario, one possibility to fulfill this gap is to downscale conventional myogenic differentiation protocols into the microfluidic environment. However, not all of these methods are compatible with the downscaling in microfluidics. For instance, enrichment of the myogenic population with sorting steps are not feasible due to the microscale dimensions of the system. Protocols that show potential for on-chip applications are those published by Shelton *et al.*, Chal *et al.*, and Xi *et al.* as they do not include cell purification passages and rely only on chemically-defined culture conditions by means of small-molecules administration. Though, small molecules-driven myogenesis presents several limitations. The efficiency of the differentiation is low, variable and lead to a final population that is highly heterogeneous [31]. Protocols are usually long (up to 50 days) and maintaining long term culture on-chip could be challenging. It becomes even more challenging considering the protocol adjustments necessary when moving to microfluidic, for example in terms of cell compatibility with the devices, media composition and frequency of media changes [32]. On the other side, differentiation protocols involving direct programming of the cells are compatible with microfluidics. In fact, microfluidic chips are proven to be the optimal devices to perform effective transfections thanks to the small ratio of medium volume to cell surface area, while also allowing for considerable costs reduction from the minimization in the quantity of reagents and compounds used [33,34]. However, it has to be considered that direct programming of hPSCs based on myogenic transcription factors administration as MYOD can be challenging. Indeed, the chromatin state in hPSCs is not permissive for the binding of MYOD to its specific sites on DNA, hampering the initiation of the myogenic transcription factors cascade. Interventions to remodel the epigenetics and the forced exit of hPSCs from their pluripotent state are therefore required to have cells prone to enter the mesoderm lineage and promote myogenic differentiation [12–14]. In this study we developed a differentiation strategy that quickly and efficiently derived human skeletal myocytes on-chip starting from hESCs and hiPSCs. Since we found that the direct on-chip administration of *MYOD* mmRNA to hESCs was not efficient in driving myogenic commitment, we decided to combine such programming strategy with a small molecules based-approach. With the absence of additional enrichment steps and targeted pluripotent gene silencing, *MYOD* mmRNA transfection-led differentiation enables fast derivation of myogenic cells, dramatically reducing experimental timings. Therefore, such strategy has the potential to considerably enhance personalized medicine applications, speeding up muscle-targeted drug development, drug screening and myopathies modelling in a transgene-free and cost-effective system.

Data and materials availability

All data is available in the main text or the supplementary materials.

Author contribution

G.S., E.S. and N.E: conception and design. G.S and E.S.: collection and assembly of data. O.G.: helped with cell culture experiments and microfluidics. PDC: helped with project development. G.S., A.U., N.E.: collection and assembly of data, data analysis and interpretation, manuscript writing. N.E.: project supervision and final approval of manuscript.

Acknowledgements

This work was supported by 2017 STARS-WiC grant of University of Padova, xProgetti di Eccellenza CaRiPaRo, TWINING of University of Padova, Oak Foundation Award (grant no. W1095/OCAY-14-191) to N.E, and by IRP Consolidator Grant 2021 (Grant Code: 21/05 Irp) to AU.

Appendix A. Supplementary data

Supplementary data related to this article can be found at https://doi.org/10.1016/j.bbrc.2021.04.129.

References

[1] Q. Wu, J. Liu, X. Wang, et al., Organ-on-a-chip: recent breakthroughs and future prospects, Biomed. Eng. Online 19 (2020).
[2] M.M. Smoak, H.A. Pearce, A.G. Mikos, Microfluidic devices for disease modeling in muscle tissue, Biomaterials 198 (2019) 250–258.
[3] J. Meseguer-Ripolles, S.R. Khetani, J.G. Blanco, et al., Pluripotent stem cell-derived human tissue: platforms to evaluate drug metabolism and safety, AAPS J. 20 (2018) 20.
[4] T. Barberi, M. Bradbury, Z. Dincer, et al., Derivation of engraftable skeletal myoblasts from human embryonic stem cells, Nat. Med. 13 (2007) 642–648.
[5] H. Sakurai, Y. Sakaguchi, E. Shoji, et al., In vitro modeling of paraxial mesodermal progenitors derived from induced pluripotent stem cells, PloS One 7 (2012), e47078.
[6] T. Hosoyama, J.V. McGivern, J.M. Van Dyke, et al., Derivation of myogenic progenitors directly from human pluripotent stem cells using a sphere-based culture, Stem Cells Transl Med 3 (2014) 564–574.
[7] B. Borchin, J. Chen, T. Barberi, Derivation and FACS-mediated purification of PAX3+/PAX7+ skeletal muscle precursors from human pluripotent stem cells, Stem. Cell. Rep. 1 (2013) 620–631.
[8] M. Shelton, A. Kocharyan, J. Liu, et al., Robust generation and expansion of skeletal muscle progenitors and myocytes from human pluripotent stem cells, Methods 101 (2016) 73–84.
[9] J. Chal, Z Al Tanoury, M. Hestin, et al., Generation of Human Muscle Fibers and Satellite-like Cells from Human Pluripotent Stem Cells in Vitro, 2016, p. 11.
[10] L. Caron, D. Kher, K.L. Lee, et al., A human pluripotent stem cell model of facioscapulohumeral muscular dystrophy-affected skeletal muscles, Stem. Cells. Transl. Med. 5 (2016) 1145–1161.
[11] H. Xi, W. Fujiwara, K. Gonzalez, et al., In vivo human somitogenesis guides

somite development from hPSCs, Cell Rep. 18 (2017) 1573–1585.
[12] S.-V. Forcales, The BAF60c-MyoD complex poises chromatin for rapid transcription, BioArchitecture 2 (2012) 104–109.
[13] S. Albini, P. Coutinho, B. Malecova, et al., Epigenetic reprogramming of human embryonic stem cells into skeletal muscle cells and generation of contractile myospheres, Cell. Rep. 3 (2013) 661–670.
[14] P.C. Toto, P.L. Puri, S. Albini, SWI/SNF-directed stem cell lineage specification: dynamic composition regulates specific stages of skeletal myogenesis, Cell. Mol. Life Sci. 73 (2016) 3887–3896.
[15] R. Darabi, R.W. Arpke, S. Irion, et al., Human ES- and iPS-derived myogenic progenitors restore DYSTROPHIN and improve contractility upon transplantation in dystrophic mice, Cell. Stem. Cell. 10 (2012) 610–619.
[16] S. Goudenege, C. Lebel, N.B. Huot, et al., Myoblasts derived from normal hESCs and dystrophic hipscs efficiently fuse with existing muscle fibers following transplantation, Mol. Ther. 20 (2012) 2153–2167.
[17] L. Rao, W. Tang, Y. Wei, et al., Highly efficient derivation of skeletal myotubes from human embryonic stem cells, Stem. Cell. Rev. Rep. 8 (2012) 1109–1119.
[18] R. Abujarour, M. Bennett, B. Valamehr, et al., Myogenic differentiation of muscular dystrophy-specific induced pluripotent stem cells for use in drug discovery, Stem Cells Transl Med 3 (2014) 149–160.
[19] S.M. Maffioletti, M.F.M. Gerli, M. Ragazzi, et al., Efficient derivation and inducible differentiation of expandable skeletal myogenic cells from human ES and patient-specific iPS cells, Nat. Protoc. 10 (2015) 941–958.
[20] M. Pawlowski, D. Ortmann, A. Bertero, et al., Inducible and deterministic forward programming of human pluripotent stem cells into neurons, skeletal myocytes, and oligodendrocytes, Stem. Cell. Rep. 8 (2017) 803–812.
[21] L. Warren, P.D. Manos, T. Ahfeldt, et al., Highly efficient reprogramming to pluripotency and directed differentiation of human cells with synthetic modified mRNA, Cell. Stem. Cell. 7 (2010) 618–630.
[22] T. Akiyama, S. Sato, N. Chikazawa-Nohtomi, et al., Efficient differentiation of human pluripotent stem cells into skeletal muscle cells by combining RNA-based MYOD1-expression and POU5F1-silencing, Sci. Rep. 8 (2018).
[23] Z.S. Badieyan, T. Evans, Concise review: application of chemically modified mRNA in cell fate conversion and tissue engineering, Stem. Cells Transl. Med. 8 (2019) 833–843.
[24] C.R. Wan, S. Chung, R.D. Kamm, Differentiation of embryonic stem cells into cardiomyocytes in a compliant microfluidic system, Ann. Biomed. Eng. 39 (2011) 1840–1847.
[25] G.G. Giobbe, F. Michielin, C. Luni, et al., Functional differentiation of human pluripotent stem cells on a chip, Nat. Methods 12 (2015) 637–640.
[26] J.M. Lee, J. Kim, E. Kang, et al., An integrated microfluidic culture device to regulate endothelial cell differentiation from embryonic stem cells, Electrophoresis 32 (2011) 3133–3137.
[28] R.L. Davis, H. Weintraub, A.B. Lassar, Expression of a single transfected cDNA converts fibroblasts to myoblasts, Cell 51 (1987) 987–1000.
[29] A. Dall'Agnese, L. Caputo, C. Nicoletti, et al., Transcription factor-directed rewiring of chromatin architecture for somatic cell nuclear reprogramming toward trans-differentiation, Mol. Cell. 76 (2019) 453–472, e8.
[30] A. Filareto, R. Darabi, R.C.R. Perlingeiro, Engraftment of ES-derived myogenic progenitors in a severe mouse model of muscular dystrophy, J. Stem Cell Res. Ther. 01 (2012), 01.
[31] J. Kim, A. Magli, S.S.K. Chan, et al., Expansion and purification are critical for the therapeutic application of pluripotent stem cell-derived myogenic progenitors, Stem. Cell. Rep. 9 (2017) 12–22.
[32] S. Halldorsson, E. Lucumi, R. Gómez-Sjöberg, et al., Advantages and challenges of microfluidic cell culture in polydimethylsiloxane devices, Biosens. Bioelectron. 63 (2015) 218–231.
[33] C. Luni, S. Giulitti, E. Serena, et al., High-efficiency cellular reprogramming with microfluidics, Nat. Methods 13 (2016) 446–452.
[34] C. Luni, E. Serena, N. Elvassore, Human-on-chip for therapy development and fundamental science, Curr. Opin. Biotechnol. 25 (2014) 45–50.